ChemPubSoc Europe

DOI: 10.1002/cbic.201800378

CHEMBIOCHEM Full Papers

Evidence of Diradicals Involved in the Yeast Transketolase Catalyzed Keto-Transferring Reactions

Ning-Shian Hsu[+],[a, b] Yung-Lin Wang[+],[a] Kuan-Hung Lin,[a, b] Chi-Fon Chang,[a] Shyue-Chu Ke,[c] Syue-Yi Lyu,[a] Li-Jen Hsu,[a] Yi-Shan Li,[a] Sheng-Chia Chen,[a] Kuei-Chen Wang,[a] and Tsung-Lin Li*[a, d]

Transketolase (TK) catalyzes a reversible transfer of a two-carbon (C_2) unit between phosphoketose donors and phosphoaldose acceptors, for which the group-transfer reaction that follows a one- or two-electron mechanism and the force that breaks the C2"–C3" bond of the ketose donors remain unresolved. Herein, we report ultrahigh-resolution crystal structures of a TK (TKps) from *Pichia stipitis* in previously undiscovered intermediate states and support a diradical mechanism for a reversible group-transfer reaction. In conjunction with MS, NMR spectroscopy, EPR and computational analyses, it is concluded that the enzyme-catalyzed non-Kekulé diradical cofactor brings about the C2"–C3" bond cleavage/formation for the C_2-unit transfer reaction, for which suppression of activation energy and activation and destabilization of enzymatic intermediates are facilitated.

Introduction

Transketolase (TK) is a thiamine diphosphate (ThDP)-dependent enzyme, which reversibly transfers a two-carbon (C_2) unit between phosphoketose donors and phosphoaldose acceptors in the pentose phosphate pathway (the PPP pathway) that is essential to almost all living organisms (Scheme 1 A).[1] Additionally, TK is of great interest in various research fields. For example, native or engineered TKs have been used as biocatalysts for the asymmetric synthesis of enantiopure ketoses by means of carboligation.[2] TK has also been considered as a drug target in several diseases, including cancers and neurodegenerative disorders.[3] The present model concerning the catalytic role of cofactor ThDP **I** (Scheme 1 B) in TK is summarized in Figure S1 in the Supporting Information.[1] This ThDP-dependent reaction is correlated to the organic N-heterocyclic carbene (NHC)-catalyzed benzoin condensation reaction; a two-electron group-transfer reaction (electron-pair transfer (EPT)).[1e,4] Given that ThDP-hydroxyethylidene radicals were reported on several occasions, for example, pyruvate:ferredoxin oxidoreductase (PFOR), pyruvate oxidase, and α-oxoglutarate dehydrogenase.[5] Given also the recent identification of enzyme-provoked non-Kekulé diradicals of thiazolium **III**′, **IV**, and **V** (Figure S2),[6] the likelihood of a single-electron transfer (SET) mechanism by TK is rekindled. The force that breaks the C2"–C3" bond of phosphoketose donors is another unresolved issue. An out-of-plane distortion of a ThDP-bound intermediate is forcefully strained due to binding-site confinement, which prevents avoiding bond-energy relaxation, and thus, suppressing dissociation energy during heterolytic cleavage of the C2"–C3" scissile bond.[7] The resulting C2"-carbanion thus substantiates umpolung chemistry (polarity inversion of the carbonyl electrophile to a nucleophile), which allows its coupling with a phosphoaldose acceptor in place. Although the reactive C2"-carbanion that forms a stable enamine (dihydroxyethylidene) intermediate has long been appreciated, this enamine is disfavorable to the reverse coupling reaction.[5b,8] Because the C2"-hydroxyethyl-ThDP carbanion appeared to be the dominant conformer in pyruvate oxidase,[5b] the existence of a stable ThDP enamine was thus questioned. Recently, the radical β,β-coupling of nitroalkenes was developed by using hydroxyethylidene thiazolium as the catalyst; this highlights the radical trait of the enamine in this coupling reaction.[9] The current model that the net condensation for a new phosphoketose necessitates an initial reverse benzoin condensation, yielding a localized C2"-carbanion to conjugate a second phosphoaldose, is subject to challenge.[1a,10] In the bid to reconcile

[a] Dr. N.-S. Hsu,[+] Dr. Y.-L. Wang,[+] K.-H. Lin, Dr. C.-F. Chang, Dr. S.-Y. Lyu, Dr. L.-J. Hsu, Dr. Y.-S. Li, Dr. S.-C. Chen, Dr. K.-C. Wang, Dr. T.-L. Li
Genomics Research Center, Academia Sinica, Taipei 115 (Taiwan)
E-mail: tlli@gates.sinica.edu.tw

[b] Dr. N.-S. Hsu,[+] K.-H. Lin
Institute of Biochemistry and Molecular Biology
National Yang-Ming University, Taipei 112 (Taiwan)

[c] Dr. S.-C. Ke
Department of Physics, National Dong Hwa University
Hualien 974 (Taiwan)

[d] Dr. T.-L. Li
Biotechnology Center, National Chung Hsing University
Taichung City 402 (Taiwan)

[+] These authors contributed equally to this work.

Supporting information and the ORCID identification numbers for the authors of this article can be found under https://doi.org/10.1002/cbic.201800378.

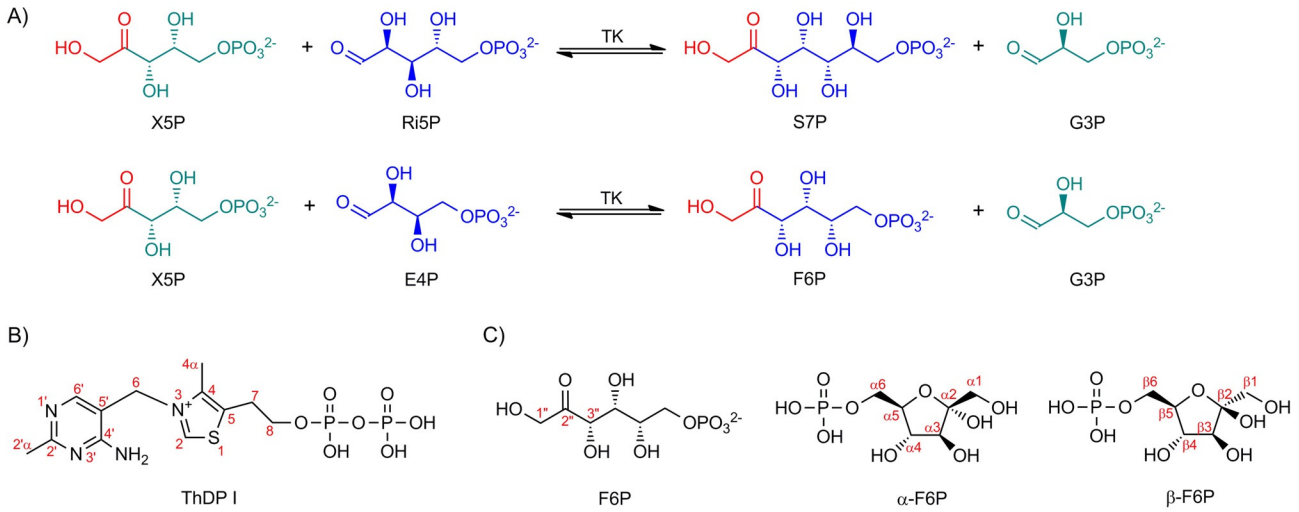

Scheme 1. TK-catalyzed reactions and chemical structures. A) Biochemical reactions catalyzed by the ThDP-dependent TK in the PPP pathway, in which a C_2-keto unit (colored red) is reversibly transferred between ketose donors (X5P/F6P/S7P) and aldose acceptors (E4P/R5P/G3P). B) Chemical structures and numbering systems for ThDP and F6P referred to herein; F6P exists in a linear or circular form in solution, of which the latter equilibrates in both α and β rotamers. X5P: D-xylulose 5-phosphate; F6P: D-fructose 6-phosphate; S7P: D-sedoheptulose 7-phosphate; E4P: D-erythrose 4-phosphate; R5P: D-ribose 5-phosphate; G3P: D-glyceraldehyde 3-phosphate; α-F6P: α-D-fructofuranose-6-phosphate; β-F6P: β-D-fructofuranose-6-phosphate.

this controversy, we have revisited TK in *Pichia stipitis* CBS6054 (TKps), an industrial strain known for its highly efficient pentose metabolism,[11] and report herein nine sub-ångström-resolution active-site structures of TKps. In conjunction with physicochemical analysis, new light was shed on the ThDP-assisted enzyme reactions, for which the reaction did not fully conform to the conventional EPT mechanism, but instead compellingly supported the SET one.

Results and Discussion

Relative energy states

The relative energy states amid the ThDP carbanion (**II**), carbene (**III**), and non-Kekulé diradicals (**III′**–**V**) were first sketched as a path coordinate (Figure 1), for which the relative energy of each isomer for its single-point energy in the gas phase was estimated by means of DFT calculations (with the Gaussian 09 suite of programs by using the B3LYP functional with a 6-31G*

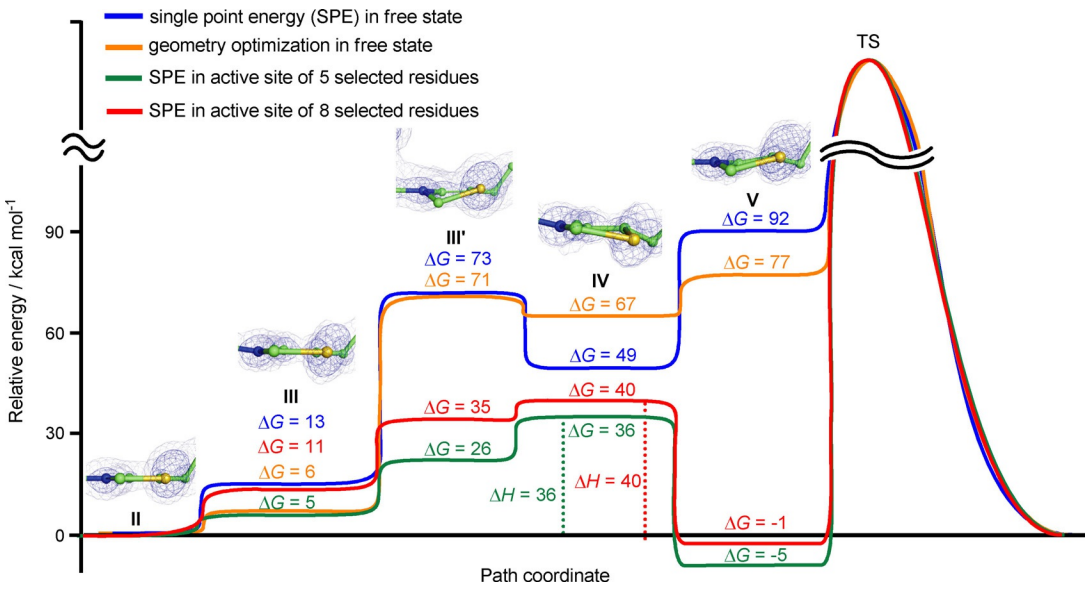

Figure 1. Reaction coordinates. The relative free energies of the ThDP carbanion (**II**), carbene (**III**), and non-Kekulé diradicals (**III′**, **IV**, **V**) are schemed as a path coordinate, for which the energy states of these ligands were estimated by DFT (with the Gaussian 09 suite of programs by using the B3LYP functional with a 6-31G* basis set, see the Supporting Information) for their single-point energy (colored blue, green, or red) and geometry optimization energy (colored orange). TS: transition state; ΔH: enthalpy change.

basis set, see the Supporting Information). Diradicals are intrinsically unstable/reactive because of their high-energy states.[12] Our calculations are consistent with this idea because the maximum free-energy difference between ThDP carbanion/carbene and diradicals is as high as about 77/92 kcal mol^{-1} (ΔH) in an enzyme-free state (Figure 1). This high-energy gap, however, can be significantly abridged if the calculation includes selected binding-site residues (Figure S3). The maximum free-energy difference (ΔH) dropped to 36/40 kcal mol^{-1}, which was less than half that without residues. Moreover, this is not a single-energy leap, but stepwise from thiazolium **II** via carbene **III** to relatively reactive **III′**/**IV** and to exothermic **V**; this suggests that the interconversion is energetically conquerable and rapid through system crossing at room temperature in TKps. We reasoned that the low effective dielectric binding site of thiazolium (Figure S4) might help shape a cagelike environment to favor back and forth or cycling conversion amid neutral, charged (carbanion/carbene), and diradical species.

Crystal complexes of TKps

Having shown how TKps overcomes "high-energy" ThDP diradicals, we then looked into the role of diradicals in the group-transfer reaction. In ternary complexes, F6P (Scheme 1C) exhibits two states freely or covalently linked to ThDP. In the free state, ThDP adapts to two different conformations bent (**VI**) or planar (**VI′**). Concerning the attacking trajectory, C2 of bent ThDP seems to position better Bürgi–Dunitz (BD) and Flippin–Lodge (FL) angles in addition to a shorter distance to C2" of F6P than that of the planar derivative (by 0.3 Å; Figure 2A and B).[13] In the linked state, three F6P–ThDP adducts (**VII**, **VIII**, and **VIII′**) exhibit unique features (Figure 2C–E): Upon olefin addition of F6P to ThDP, the C2"–C3" bond is perpendicular to the thiazolium plane, which is in accordance with the principle of "maximum overlap orbital" favorable for heterolytic bond cleavage (Figure S1).[14] In **VII**, S1 (bent thiazolium) surprisingly lies above the plane defined by the planar thiazolium, in contrast to F6P–ThDP reported by Tittmann et al.,[7,15] for which the thiazolium ring is planar. This phenomenon is not limited to F6P, but extended to X5P (Figure S5G). Concerning the bond length, both C2–C2" and C2"–C3" are almost identical (1.54 Å; Figure 2C), which indicates that these two bonds are less strained. The thiazolium ring reinstates its planarity in **VIII** and **VIII′**, whereas the C2–C2" bond is placed down the plane and is likely to be subject to binding-site confinement, as proposed by Tittmann et al.,[7] which implies that losing/gaining aromaticity has a role in the leverage of the C2"–C3" bond length. Moreover, the bond lengths in both C2–C2" and C2"–C3" are unequal, with one longer than the other in a dynamic manner (Figure 2D and E). The bent (diradical) F6P-thiazolium

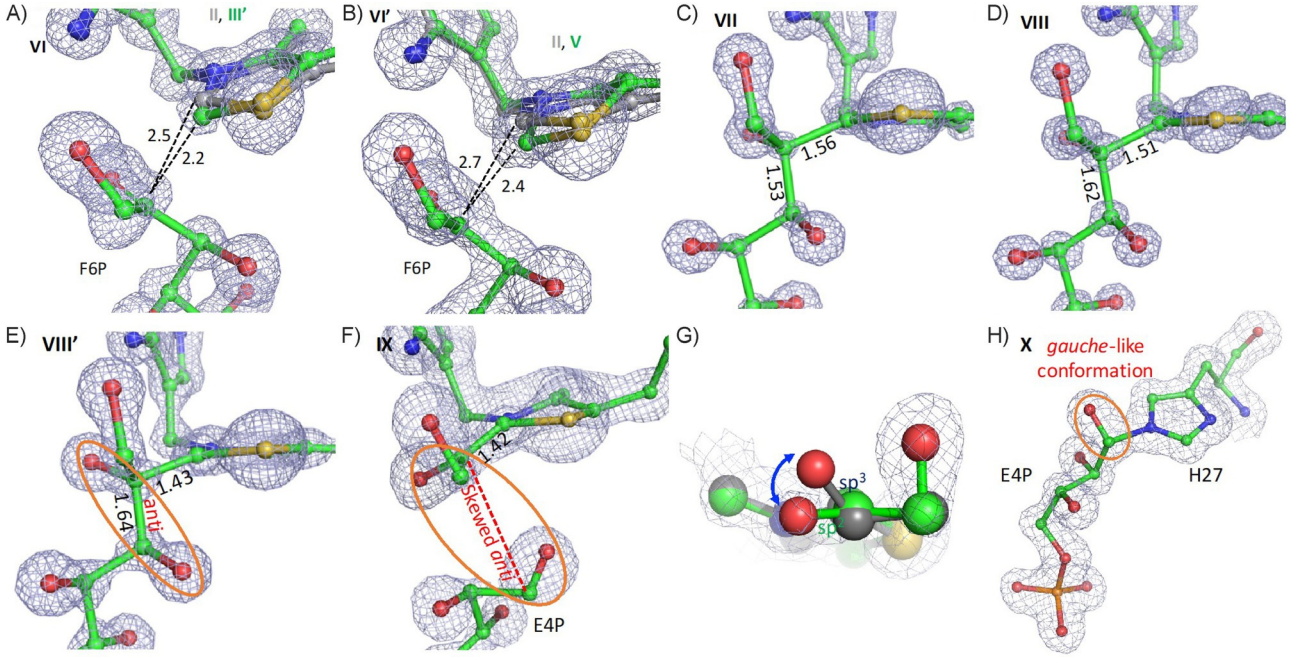

Figure 2. Ligands in the active site of TKps. A) **VI**: C2 of planar ThDP or bent ThDP **III′** is poised to attack C2" of F6P through the one- or two-electron mechanisms, respectively, for which the distance between C2 and C2" with bent ThDP **III′** is shorter than that with the planar one by 0.2 Å. B) **VI′**: The distance between C2 and C2" with bent ThDP **V** is shorter than that with the planar one by 0.3 Å. C) **VII**: ThDP and F6P are associated through a covalent linkage. The adduct is in a relaxed state, in which the bent thiazolium exhibits equal bond lengths for C2–C2" (1.56 Å) and C2"–C3" (1.53 Å). D) **VIII**: ThDP and F6P are associated through a covalent linkage. The adduct is in an energetic state, for which the planar thiazolium exhibits unequal bond lengths for C2–C2" (1.51 Å) and C2"–C3" (1.55 Å). E) **VIII′**: ThDP and F6P are associated through a covalent linkage. The adduct is in an energetic state, in which the planar thiazolium exhibits unequal bond lengths for C2–C2" (1.46 Å) and C2"–C3" (1.64 Å). F) **IX**: Structural view of E4P-DHE-ThDP, in which the thiazolium is bent and a radical is likely vested in C2" (a diradical species). The aldehyde group of E4P adapts a skewed *anti* configuration, relative to C2"–OH. G) Superposition of dihydroxyethylidene (colored green; this study, PDB ID: 5XU9) and hydroxylethyl-thiazolium (colored gray; PDB ID: 4FEG), in which C2" takes an sp^2 or sp^3 configuration in the former or the latter, respectively. H) **X**: Holo-TKps soaked with E4P, in which E4P takes a *gauche*-like conformation in close proximity to H27. The $2F_o-F_c$ electron density map is contoured at 2σ, unless otherwise specified (see Figure S5 for the F_o-F_c difference omit maps and stereoviews). The figures shown in the structures are bond lengths for the bonds specified in Å.

in **VII** seems to be more "energetically relaxed" than that (planar) in **VIII**/**VIII**′. If radicals are involved in the group-transfer reaction, radicals should not be limited to thiazolium, but spread to other parts of the adduct. This reasoning, however, contradicts the current model that thiazolium retains planarity throughout the reaction course before/after the C2 carbanion/carbene nucleophilically attacks the C2" electrophile. Nonetheless, the bond lengths in dynamics denote that the resonance energy is conveyed to the C2–C2"–C3" bond if bent thiazolium reverts back to being planar. We thus hypothesize that this isomeric ring bending, along with F6P-ThDP being strained in the binding site, are critical factors that facilitate breakage of the C2"–C3" bond.

Diradical model for TKps

A quaternary complex (**IX**) was further obtained in crystals soaked with F6P, for which F6P has been converted into a C_2-keto unit dihydroxylethyl (DHE) covalently linked to ThDP (DHE-ThDP) with a phosphoaldose E4P in close proximity to DHE in a bond association/dissociation manner (Figure 2F). This DHE moiety is dissimilar to hydroxylethyl-ThDP reported by Tittmann et al.,[5b] in which C2" is of sp^3 type with a C2"–C2 bond length of 1.52 Å (Figure 2G). In contrast, C2" in **IX** assumes an sp^2-like configuration with a C2"–C2 bond length of 1.42 Å (≈1.5 bond order); this implies that the adduct is the long-sought-after dihydroxyethylidene (Breslow) intermediate or a DHE-thiazolium diradical species (one is a nonbonding σ-type radial at C2" (sp^2) and the other is a π-type radical at thiazolium). Additionally, the aldehyde group of E4P is posed in a skewed *anti* configuration, relative to C2"-OH of DHE. This group in a binary crystal soaked with E4P (**X**), however, takes a *gauche*-like configuration in close proximity to the imidazole ring of H27 (Figure 2H), thus suggesting that H27 is in a position to orientate/stabilize E4P/ketose-ThDP during C2"–C3" bond cleavage/formation. Given the traditional model (two-electron reaction), the C2" carbanion of DHE-ThDP attacks the C3" carbonyl carbon of a phosphoaldose, for which the HOMO of the nucleophile fits the LUMO of the unsaturated trigonal center of the electrophile.[13,16] Given that DHE-ThDP is a diradical as a whole, its coupling with E4P through the singly occupied molecular orbital (SOMO) chemistry fits as well as that of the HOMO/LUMO (C2"-carbanion/C3"-aldehyde) counterpart (Figure S1). In this context, C2"=O would degenerate to a ketyl radical species (C2"–O•) upon the SOMO-type association (Scheme 2).

As shown in **VII**/**VIII**/**VIII**′, both C2"–OH and C3"–OH adopt an *anti*-like configuration with an angle and distance that allow C2"–O• to abstract a vicinal H atom at C3". With the assistance of H27, the resulting C3"• species may bring about the homolytic cleavage of C2"–C3" in addition to the above-mentioned factors. In the reverse reaction (forming a new C2"–C3" bond), C2"• of a DHE-ThDP diradical may likewise pair with the aldehyde group of E4P to form C3"–O•. Given that both C2"–OH of DHE-ThDP and C3"-O• of E4P may align in a *gauche*-like configuration, C3"–O• is thus in a position to abstract the adjacent H atom of C2"–OH to form a C2"–O• species. This radical species then reconfigures to form C2"=O in concert with homolytic cleavage of the C2"–C2 bond, whereby F6P/S7P/X5P is reversely detached from ThDP. Collectively, a radical C_2-transferring reaction is proposed (Scheme 1). The reaction begins with attack of a ThDP diradical to a phosphoketose, which results in an oxo radical species at C2". This species then abstracts the (*S*)-H atom at C3" to form a C3"• species. If the bent thiazolium regains its aromaticity, the bond energy of C2"–C3" is weakened due to resonance energy relay, spatial confinement, and stabilizing/polarizing effects of H27. The C2"–C3" bond is thereby homolytically cleaved into two n/σ radicals at C2" and C3". The former either localizes as a C2" carbanion or resonances to form a DHE-ThDP/non-Kekulé diradical. The latter ends up as an aldehyde through orbital reconfiguration. In the reverse reaction, C2"• of the DHE-ThDP diradical may prime the reaction with a *gauche*-like aldose (E4P/Ri5P/G3P) oriented at the helm of H27 to complete the benzoin condensation for a new phosphoketose.

Model validation

To validate this working model, we performed a deuterium-exchange experiment with F6P as a single substrate. The fact is that deuterium(s) should be incorporated into F6P if the reaction follows SOMO chemistry, or it would otherwise support classical HOMO/LUMO chemistry. Holo-TKps and F6P (M_w = 259) were incubated in a deuterium oxide buffer solution (Tris 20 mM, NaCl 100 mM, pH 7.5) and subjected to MS analysis in due course (16 h). Biochemical analysis revealed that the molecular weight of F6P in the presence of holo-TKps was increased, interestingly not by one, but by multiple atomic mass units (M_w = 259–266; Figure 3A). Given that the increment of mass units may be subject to keto/enol tautomerization or α/β rotamerization in solution, this possibility, however, was ruled out because the molecular weight of F6P did not change if the reaction was conducted in a deuterium buffer solution (Tris 20 mM, NaCl 100 mM, pH 7.5) containing apo-TKps (no ThDP) under the same conditions. Additionally, ^{1}H NMR spectroscopic analysis was conducted for F6P in a D_2O or H_2O buffer solution (deuterated Tris 20 mM, pH 7.5) with holo-TKps, in which the proton signal areas of F6P in D_2O decreased with time elapsed, as opposed to those of F6P in H_2O, which remained almost constant (Figures 3B and S6). HSQC NMR spectroscopic analysis further confirmed that protons in both experiments were well correlated to the same carbon atoms of F6P (Figure S6); thus indicating a consequence of radical scrambling. There are some unassigned minor signals in the NMR spectra, which may be ascribed to isomers of F6P/E4P that are likely to be due to radical-induced racemization. Concerning direct detection of organic radicals of ThDP in TKps, holo-TKps was subjected to EPR analysis; electron spins in the EPR spectrum were barely detected. The weak signal may be attributed to sensitivity to dioxygen, rapid interconversion and/or dipole interference (spins are too close) amid n/π orbitals of diradicals, in that net electron spins in the triplet paramagnetic state (↑↑) were attenuated by those in the silent singlet diamagnetic state (↑↓). Nonetheless, a significant EPR signal was detected at g = 2.13

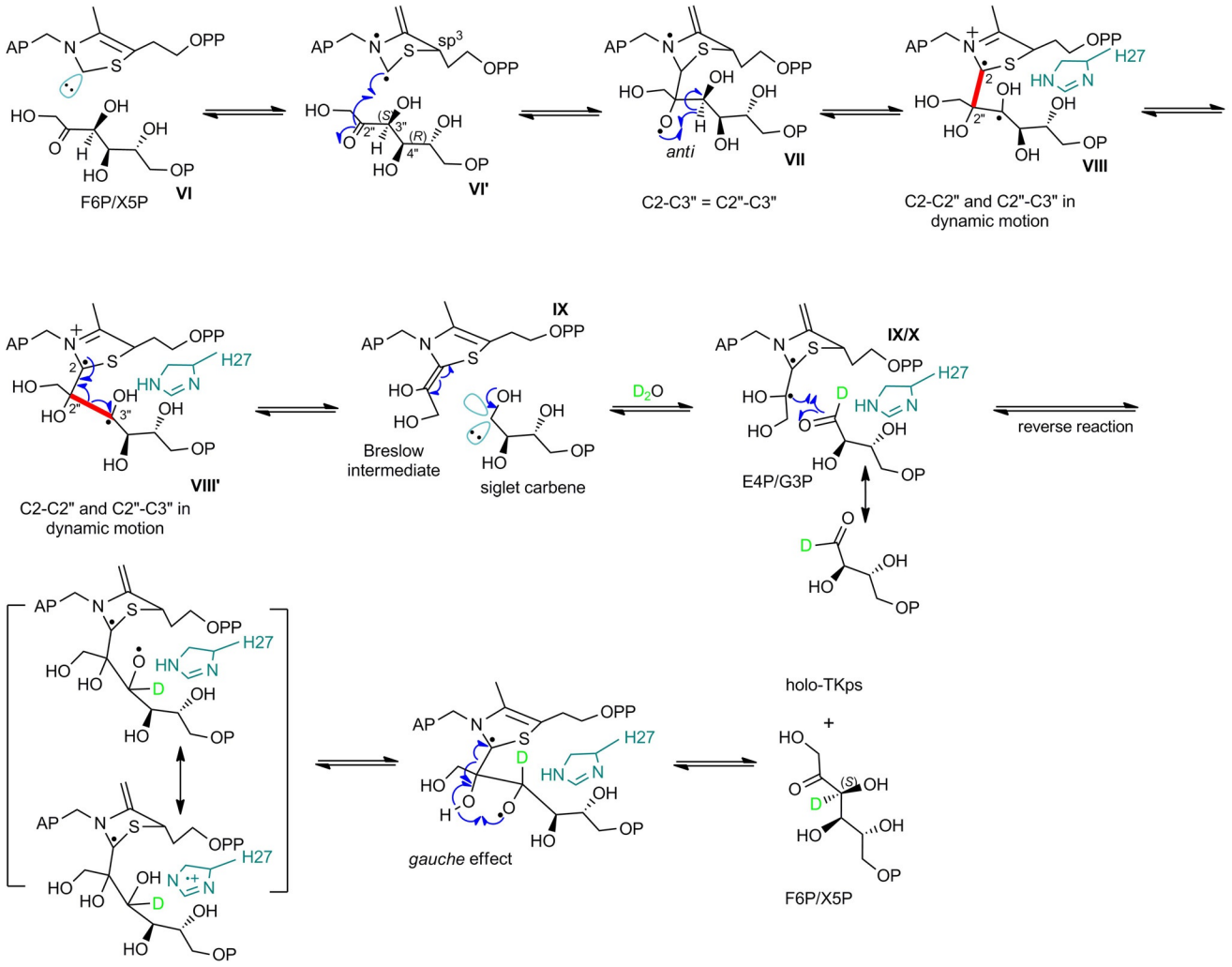

Scheme 2. Proposed SET mechanism. See the main text for details. Given this mechanism, deuterium substitution in F6P should primarily end up at the position in green.

in a dose-dependent manner for the sample containing F6P (Figure 3C). The *g* value is atypical and unexpected (more broadening and away from the free electron signal), which suggests that a spin dipole is coupled to another paramagnetic spin dipole, possibly with a different relaxation time in TKps. To confirm that the signal is directly related to the spins in the active site, we performed EPR experiments with enzymatically synthesized [$^{13}C_6$]F6P, whereby spin signals display unique hyperfine splitting ($g = 2.038$, $A = 80$ G); this confirms that electron spins interact with ^{13}C nuclei of F6P in TKps. As described above, that E4P is in close proximity to H27 (Figure 2H), H27 was considered to play an important role in the stabilization/initialization of radicals during the cleavage/formation of the C2"–C3" bond for a resulting ketose-ThDP or aldose–phosphate. Given TKps H27A/C, the spin signal almost vanished; this is in agreement with the spin-coupled ensemble being related to the proposed functionalities of H27 (Scheme 1). Taken together, a TKps-catalyzed group-transfer reaction that follows the SET mechanism is evident, whereas the reaction in concert with EPT cannot be excluded at the current stage.

In light of the solved complexes, both the bent thiazolium adduct, which shows equal bond lengths in C2–C2"–C3", and the planar adduct, which shows unequal bond lengths, support a sequence of resonance energy relay. The calculated energy of 36–40 kcal mol^{-1} accounts for the resonance energy between a planar and a bent thiazolium, which correlates the energy needed for 0.1–0.2 Å bond elongation.[17] Given that the bond elongation of 0.09–0.11 Å (from 1.53 to 1.62–1.64 Å) is tantamount to a deduction of 35/40 kcal mol^{-1} of dissociation energy,[14c,d] the ring bending effect thus considerably offsets endothermic cleavage of the C–C bond. The benzoin condensation is known to be more favorable for bond formation, but less favorable for bond cleavage. Concerning simplicity for a reversible chemical reaction, SET seems to outstrip EPT. Both SET and EPT, nonetheless, meet the concepts proposed by Pauling that rate accelerations for enzymatic reactions arise from high specificity of biocatalysts through stabilizing transition-state complexes and repressing activation energies,[18] as well as by Albery and Knowles, who reported that both activated substrates and destabilized intermediates with comparable free energy were crucial for enzymes to carry out reactions.[19]

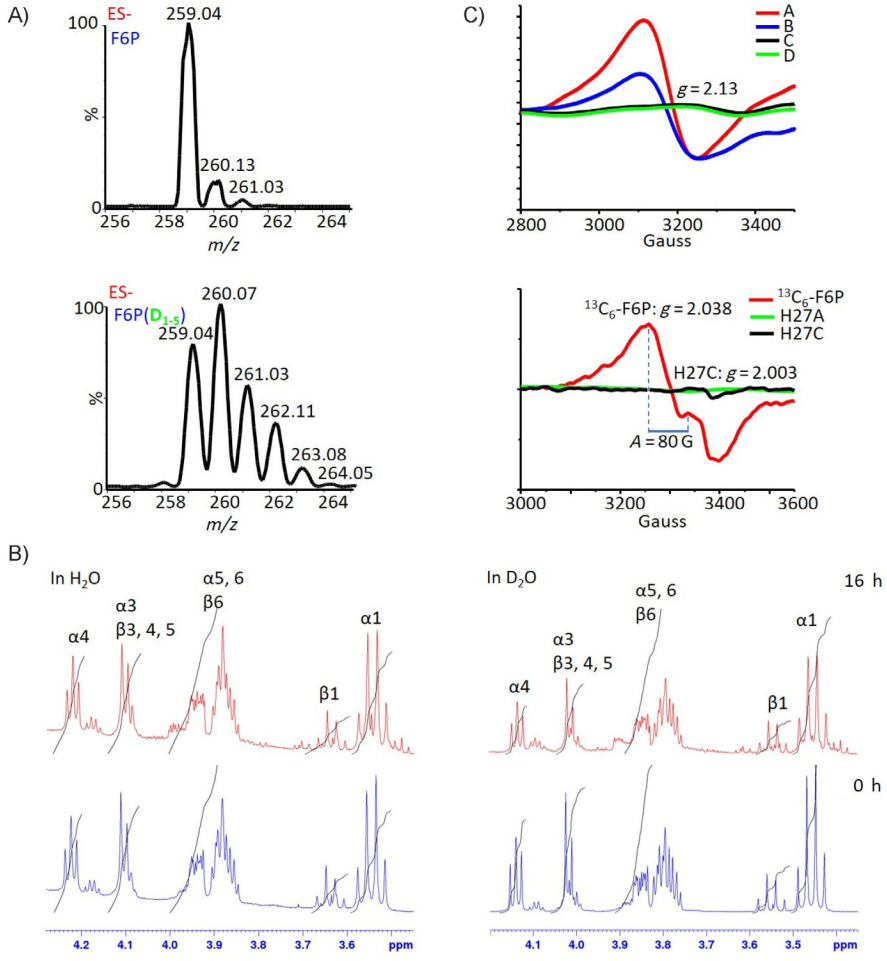

Annotation	Relative peak area in H_2O		% reduction
	0 h	16 h	
α1	1	1	0
β1	0.39	0.37	5.1
α5, 6 β6	2.57	2.50	2.7
α3 β3, 4, 5	1.04	0.99	4.8
α4	0.96	0.96	0

Annotation	Relative peak area in D_2O		% reduction
	0 h	16 h	
α1	1	1	0
β1	0.24	0.24	0
α5, 6 β6	2.02	1.92	4.4
α3 β3, 4, 5	0.66	0.51	24
α4	0.49	0.34	31

Figure 3. A) Mass spectra of F6P in the presence of apo-TKps (without ThDP, top) or holo-TKps (with ThDP, bottom) incubated in a deuterium oxide buffer solution for 90 min, in which the isotopic profile of F6P in the sample containing holo-TKps shows incorporation of multiple deuterons (ES^-: negative mode). B) ^1H NMR spectra of F6P for the samples containing holo-TKps and incubated in a water (left) or deuterium oxide (right) buffer solution for 16 h, in which hydrogen atoms of F6P in D_2O were significantly replaced by deuterons as the relative ratio of hydrogen atoms decreased with time (F6P forms both cyclic α- and β-furanose anomers (major) and a linear isomer (minor) in solution; signal areas were compared because of signal multiplicity). C) Top: EPR spectra of holo-TKps in the presence (A, B; the concentration of A is twice that of B) or absence (C; no F6P) of F6P and the control (D; ThDP plus F6P without TKps); bottom: EPR spectra of holo-TKps in the presence of [$^{13}C_6$]F6P (red) or H27A (green)/H27C (black) in the presence of F6P (*g*/*A* values are designated, which were determined by using Bruker's software SimFonia-WinEPR).

Conclusion

The bent thiazolium and its ketose adducts identified herein were unrelated to the oxidative SET process of PFOR because there was no net gain/loss of electrons from both thiazolium mesomerism and the group-transfer reaction. The structural information in conjunction with physicochemical evidence leads us to come up with a diradical mechanism for TKps, which indeed meets all catalytic criteria, particularly concerning the efficient C2"–C3" bond cleavage/formation of phosphoketoses. Although the conventional EPT mechanism, with several mechanistic merits, has prevailed for years, the mechanism, however, cannot reconcile the high energy demand for C2"–C3" bond cleavage/formation and for facile reversible group-transfer reactions. Additionally, the formation of a nucleophilic C2 carbene/carbanion is the key step in the forward reaction to initiate the C2"–C3" bond cleavage of a donor phosphoketose; the formation of a localized C2" carbanion, however, is the key

step in the reverse reaction to trigger C2″–C3″ bond formation for a distinctive phosphoketose. In terms of reactivity, diradical conformers (**III′**/**IV**) are more reactive than carbanion/carbene counterparts (**II**/**III**) on the basis of the potential-energy landscape (Figure 1), which makes SET a more favorable mechanism than that of EPT. Likewise, hydroxyethylidene thiazolium type catalysts are known/used as decent radical initiators in both biochemical and organic reactions, further proving that SET is a more favorable mechanism. Considering the coexistence of the C2 carbanion/carbene and the localized C2″ carbanion, EPT in parallel with SET cannot be ruled out. Nonetheless, the active-site geometry and/or environment in TKps seemingly favors mesomerism of the thiazolium ring to its neutral, charged, or diradical alternatives in a dynamic manner likely through rapid thermal crossing and a captodative effect. Beyond this, desolvation in the cofactor/substrate binding site with a low effective dielectric constant is likewise cooperative for electron hopping/relay.[6] The π radicals of thiazolium are in a position to trigger the breakage/formation of the C2″–C3″ bond; thus facilitating the interconversion of phosphoketoses by virtue of this diradical mechanism. To this end, the overall entropy gains upon the phosphoketose-ThDP-TKps tripartite interplay should substantially complement endothermic bond lengthening or bond cleavage. This analysis is in line with the Circe effect,[20] because the high activation-energy barriers between transition states and ground states of intermediates are decomposed to a discrete energy landscape of isomers of intermediates; thus easing C–C bond breakage/formation. Finally, the multiple complexes and the mechanism disclosed herein can serve as a working model for future quantitative kinetics and computational validation by using a quantum mechanical/molecular mechanical method. The new concept may also be applicable to some other ThDP-dependent enzymes for attractive prospects in biocatalytic applications and/or drug design.

Experimental Section

Cloning and protein purification: The cloning and protein purification of TKps followed standard protocols.[6] In brief, the *tkt1* gene was amplified from *P. stipitis* CBS6054 genomic DNA by PCR and subcloned into the expression vector pET-28a (+). The expression plasmid that afforded N-terminally His_6-tagged proteins was then transformed into *E. coli* BL21(DE3) cells by electroporation and then grown on lysogeny broth (LB) agar plates containing 50 μg mL^{-1} kanamycin for 16 h at 37 °C. A single colony was grown overnight in LB medium (5 mL) containing 50 μg mL^{-1} kanamycin at 37 °C. The cell culture was used to inoculated LB medium (1 L) containing kanamycin (50 mg L^{-1}). Protein expression was induced with isopropyl-β-D-thiogalactopyranoside (200 μL; 1.0 M) at an OD_{600} of 0.6, and grown for a further 24 h at 16 °C. Cells were harvested by centrifugation, resuspended in binding buffer (20 mL; 20 mM Tris at pH 8.0, 500 mM NaCl, 10 mM imidazole, 10% glycerol), and ruptured by microfluidizer/sonication. The cell-free extract was centrifuged at 17000 rpm (34957 *g*) for 30 min, and the supernatant was applied to an Ni^{2+}-NTA resin column. The column was sequentially washed with binding buffer and wash buffer (20 mM Tris at pH 8, 500 mM NaCl, 80 mM imidazole). The bound protein was then eluted with elution buffer (10 mL; 20 mM Tris at pH 8, 500 mM NaCl, 250 mM imidazole). The yield of protein was about 10 mg L^{-1}, of which the enzymatic activity was examined by using the conventional enzyme-coupled assay (triosephosphate isomerase and glycerol-3-phosphate dehydrogenase) to monitor the production/consumption of G3P.[21] Gel filtration was performed by using an Äkta FPLC system equipped with an S-200 Superdex column (Amersham Bioscience) under isocratic conditions (20 mM Tris, pH 8, 100 mM NaCl).

Crystallization and data collection: The purified proteins were crystallized by using the hanging drop vapor-diffusion method. TKps was concentrated to 20 mg mL^{-1} and crystalized in a solution containing: 0.1 M MES at pH 6.5, 0.1 M NaCl, 30% (*v*/*v*) poly(ethylene glycol) (PEG) 400 at 20 °C. Crystals appeared within 5 days and exhibited diffraction consistent with the space group $C222_1$. TKps–ThDP binary complexes were obtained in a solution containing 0.1 M MES at pH 6.5, 0.1 M NaCl, 30% (*v*/*v*) PEG 400, and 5 mM ThDP. For the ternary complexes, the TKps–ThDP binary crystals were soaked with substrates (X5P/F6P/R5P/E4P, 5 mM) dissolved in the same solution for 3–40 min. For the complex **IX** (containing DHE-ThDP and E4P), two ternary crystals were obtained from dozens of TKps–ThDP binary crystals soaked with 5 mM F6P for 5–10 min. Complex **X** (containing E4P) was obtained from soaking TKps–ThDP binary crystals with E4P (2 mM) for 15 min. XRD data sets were collected on ADSC Quantum-315 or MX300HE CCD detectors at beamlines 13B1, 13C1, 15A1, and 05A of the National Synchrotron Radiation Research Center (Taiwan), or at beamline 44XU of Spring-8 (Japan).

Deuterium exchange of F6P: Reactions containing F6P (2 mM) in 95% deuterium oxide or 100% water Tris buffer solution were initiated by the addition of holo-TKps (0.25 mM) at 25 °C for 0 and 16 h. The reactions, in due course, were quenched by chloroform, from which the insoluble portion was removed by using a centrifugal filter unit. The filtrate was lyophilized under a free dryer. The dried samples were then resuspended in D_2O for NMR spectroscopic analysis or in H_2O for LC-MS analysis.

LC-MS analysis: LC-MS analysis was performed with a reversed-phase column (VyDAC-C_{18} column, 5 μm; 4.6×250 mm) linked on a Waters Alliance 2695 HPLC module, in connection with a Xevo TQ-S micro triple quadrupole mass spectrometer, at a flow rate of 1 mL min^{-1} solvent solution, which contained water and acetonitrile with 0.1% formic acid. The analytes were eluted with 98% water followed by a linear gradient of 2 to 98% acetonitrile, and finally the column was equilibrated back to 98% water.

NMR spectroscopy: Compounds ThDP and F6P were purchased from Sigma–Aldrich. All NMR spectroscopic analyses were performed on Bruker Avance 600 spectrometers equipped with a CryoProbe. The 1D ^1H and ^{13}C and 2D HSQC spectra were recorded at 298 °K by using deuterated buffer solutions (deuterated Tris 20 mM at pH 7.5 in D_2O or in H_2O with 10% D_2O for water signal suppression) for analysis. NMR spectroscopy data were analyzed by using the TopSpin software (version 3.5). ^1H NMR chemical shifts are reported in units of ppm relative to tetramethylsilane (see Figure S6 for the NMR spectra). F6P: ^1H NMR (600 MHz, D_2O): $\delta = 3.48$ (dd, $J = 12.0$, 13.5 Hz, 2H), 3.83–3.94 (m, 4H), 4.16 (d, $J = 7.8$ Hz, 1H), 4.23 ppm (t, $J = 7.6$ Hz, 1H); ^{13}C NMR (150 MHz, D_2O): $\delta = 62.6$ (C1), 64.2 (C6), 74.4 (C4), 75.2 (C3), 79.9 (C5), 101.4 ppm (C2)

EPR spectroscopy: EPR spectra were obtained by using a Bruker EMX X-band (Bruker Biospin) instrument at the X band (9.2 GHz). The *g*/*A* values were determined by using the Bruker software SimFonia-WinEPR. A typical sample that contained 0.5 mM holo-TKp/H27A/H27C, 1 mM ThDP, and 3 mM F6P (dissolved in 20 mM Tris

buffer at pH 7.5) was loaded into an EPR sample tube and then frozen in a standard liquid-helium immersion Dewar to maintain the temperature at 5 K for data collection. ^{13}C-labeled F6P was enzymatically synthesized by using hexokinase in the presence of ^{13}C-labeled fructose and adenosine triphosphate (ATP). The mass spectrum of [$^{13}C_6$]F6P is shown in Figure S7.

Enzymatic synthesis of [$^{13}C_6$]F6P: The conversion of [$^{13}C_6$]fructose into [$^{13}C_6$]F6P was completed by using hexokinase at 25 °C and pH 7.5 with ATP and Mg^{2+} as cosubstrates. In brief, the enzymatic reaction in a buffer solution (20 mM Tris) containing [$^{13}C_6$]fructose (2 mM), $MgCl_2$ (2.5 mM), and ATP (2 mM) was initiated with the addition of an appropriate amount of hexokinase (1 U, total volume 3.0 mL) overnight. The yield of [$^{13}C_6$]F6P was about 50%, which was purified by HPLC for use. All compounds and hexokinase were purchased from Sigma Aldrich.

PDB accession codes: The atomic coordinates have been deposited in the Protein Data Bank with the IDs 5XU2, 5XRV, 5XTX, 5XT0, 5XT4, 5XU9, 5XPS, 5XQK, and 5XQA.

Acknowledgements

This work was supported by funds from the Ministry of Science and Technology (104-0210-01-09-02, 105-2627-M-001-008, and 106-2627-M-001-007) and Academia Sinica. We thank both the National Synchrotron Radiation Research Center of Taiwan and SPring-8 of Japan for beam time allocations at beam lines 13C, 13B, 15A, 05A, 12B2, and 44XU. We thank Dr. Steve Sheng-Fa Yu of the Institute of Chemistry for assistance performing EPR.

Conflict of Interest

The authors declare no conflict of interest.

Keywords: C–C coupling · electron transfer · enzyme catalysis · radical reactions · reaction mechanisms

[1] a) P. Neumann, K. Tittmann, *Curr. Opin. Struct. Biol.* **2014**, *29*, 122–133; b) K. Schröder-Tittmann, D. Meyer, J. Arens, C. Wechsler, M. Tietzel, R. Golbik, K. Tittmann, *Biochemistry* **2013**, *52*, 2505–2507; c) R. Kluger, K. Tittmann, *Chem. Rev.* **2008**, *108*, 1797–1833; d) D. Kern, G. Kern, H. Neef, K. Tittmann, M. Killenberg-Jabs, C. Wikner, G. Schneider, G. Hubner, *Science* **1997**, *275*, 67–70; e) A. Balakrishnan, Y. Gao, P. Moorjani, N. S. Nemeria, K. Tittmann, F. Jordan, *J. Am. Chem. Soc.* **2012**, *134*, 3873–3885; f) N. Nemeria, S. Chakraborty, A. Baykal, L. G. Korotchkina, M. S. Patel, F. Jordan, *Proc. Natl. Acad. Sci. USA* **2007**, *104*, 78–82; g) F. Jordan, *FEBS Lett.* **1999**, *457*, 298–301.

[2] a) N. J. Turner, *Curr. Opin. Biotechnol.* **2000**, *11*, 527–531; b) C. U. Ingram, M. Bommer, M. E. B. Smith, P. A. Dalby, J. M. Ward, H. C. Hailes, G. J. Lye, *Biotechnol. Bioeng.* **2007**, *96*, 559–569; c) D. Gocke, L. Walter, E. Gauchenova, G. Kolter, M. Knoll, C. L. Berthold, G. Schneider, J. Pleiss, M. Muller, M. Pohl, *ChemBioChem* **2008**, *9*, 406–412; d) N. Nemeria, E. Binshtein, H. Patel, A. Balakrishnan, I. Vered, B. Shaanan, Z. Barak, D. Chipman, F. Jordan, *Biochemistry* **2012**, *51*, 7940–7952; e) M. Levine, C. S. Kenesky, D. Mazori, R. Breslow, *Org. Lett.* **2008**, *10*, 2433–2436; f) D. Meyer, L. Walter, G. Kolter, M. Pohl, M. Muller, K. Tittmann, *J. Am. Chem. Soc.* **2011**, *133*, 3609–3616; g) H. C. Hailes, D. Rother, M. Muller, R. Westphal, J. M. Ward, J. Pleiss, C. Vogel, M. Pohl, *FEBS J.* **2013**, *280*, 6374–6394.

[3] a) Y. Le Huerou, I. Gunawardana, A. A. Thomas, S. A. Boyd, J. de Meese, W. Dewolf, S. S. Gonzales, M. Han, L. Hayter, T. Kaplan, C. Lemieux, P. Lee, J. Pheneger, G. Poch, T. T. Romoff, F. Sullivan, S. Weiler, S. K. Wright, J. Lin, *Bioorg. Med. Chem. Lett.* **2008**, *18*, 505–508; b) J. Zhao, C. J. Zhong, *Neurosci. Bull.* **2009**, *25*, 94–99; c) V. I. Bunik, A. Tylicki, N. V. Lukashev, *FEBS J.* **2013**, *280*, 6412–6442; d) D. X. Liu, Z. J. Ke, J. Luo, *Mol. Neurobiol.* **2017**, *54*, 5440–5448; e) C. W. Tseng, W. H. Kuo, S. H. Chan, H. L. Chan, K. J. Chang, L. H. Wang, *Cancer Res.* **2018**, *78*, 2799–2812.

[4] a) R. Breslow, *J. Biol. Chem.* **2009**, *284*, 1337–1342; b) O. Hollóczki, Z. Kelemen, L. Nyulaszi, *J. Org. Chem.* **2012**, *77*, 6014–6022; c) A. Berkessel, S. Elfert, K. Etzenbach-Effers, J. H. Teles, *Angew. Chem. Int. Ed.* **2010**, *49*, 7120–7124; *Angew. Chem.* **2010**, *122*, 7275–7279.

[5] a) N. S. Nemeria, A. Ambrus, H. Patel, G. Gerfen, V. Adam-Vizi, L. Tretter, J. Zhou, J. Wang, F. Jordan, *J. Biol. Chem.* **2014**, *289*, 29859–29873; b) D. Meyer, P. Neumann, E. Koers, H. Sjuts, S. Ludtke, G. M. Sheldrick, R. Ficner, K. Tittmann, *Proc. Natl. Acad. Sci. USA* **2012**, *109*, 10867–10872; c) E. Chabriere, X. Vernede, B. Guigliarelli, M. H. Charon, E. C. Hatchikian, J. C. Fontecilla-Camps, *Science* **2001**, *294*, 2559–2563.

[6] N. S. Hsu, Y. L. Wang, K. H. Lin, C. F. Chang, S. Y. Lyu, L. J. Hsu, Y. C. Liu, C. Y. Chang, C. J. Wu, T. L. Li, *Angew. Chem. Int. Ed.* **2018**, *57*, 1802–1807; *Angew. Chem.* **2018**, *130*, 1820–1825.

[7] S. Lüdtke, P. Neumann, K. M. Erixon, F. Leeper, R. Kluger, R. Ficner, K. Tittmann, *Nat. Chem.* **2013**, *5*, 762–767.

[8] G. Wille, D. Meyer, A. Steinmetz, E. Hinze, R. Golbik, K. Tittmann, *Nat. Chem. Biol.* **2006**, *2*, 324–328.

[9] Y. Du, Y. H. Wang, X. Li, Y. L. Shao, G. H. Li, R. D. Webster, Y. R. Chi, *Org. Lett.* **2014**, *16*, 5678–5681.

[10] A. Vrielink, N. Sampson, *Curr. Opin. Struct. Biol.* **2003**, *13*, 709–715.

[11] a) S. H. Chen, D. R. Hwang, G. H. Chen, N. S. Hsu, Y. T. Wu, T. L. Li, C. H. Wong, *ACS Chem. Biol.* **2012**, *7*, 481–486; b) T. W. Jeffries, I. V. Grigoriev, J. Grimwood, J. M. Laplaza, A. Aerts, A. Salamov, J. Schmutz, E. Lindquist, P. Dehal, H. Shapiro, Y. S. Jin, V. Passoth, P. M. Richardson, *Nat. Biotechnol.* **2007**, *25*, 319–326.

[12] M. Abe, *Chem. Rev.* **2013**, *113*, 7011–7088.

[13] H. B. Burgi, J. D. Dunitz, J.-M. Lehn, G. Wipff, *Tetrahedron* **1974**, *30*, 1563–1572.

[14] a) M. H. Charon, A. Volbeda, E. Chabriere, L. Pieulle, J. C. Fontecilla-Camps, *Curr. Opin. Struct. Biol.* **1999**, *9*, 663–669; b) E. Chabriere, M. H. Charon, A. Volbeda, L. Pieulle, E. C. Hatchikian, J. C. Fontecilla-Camps, *Nat. Struct. Bio.l* **1999**, *6*, 182–190; c) N. Matsunaga, D. W. Rogers, A. A. Zavitsas, *J. Org. Chem.* **2003**, *68*, 3158–3172; d) A. A. Zavitsas, *J. Phys. Chem. A* **2003**, *107*, 897–898.

[15] D. Meyer, P. Neumann, R. Ficner, K. Tittmann, *Nat. Chem. Biol.* **2013**, *9*, 488–490.

[16] G. J. Bartlett, A. Choudhary, R. T. Raines, D. N. Woolfson, *Nat. Chem. Biol.* **2010**, *6*, 615–620.

[17] P. Asztalos, C. Parthier, R. Golbik, M. Kleinschmidt, G. Hubner, M. S. Weiss, R. Friedemann, G. Wille, K. Tittmann, *Biochemistry* **2007**, *46*, 12037–12052.

[18] L. Pauling, *Nature* **1948**, *161*, 707–709.

[19] W. J. Albery, J. R. Knowles, *Angew. Chem. Int. Ed. Engl.* **1977**, *16*, 285–293; *Angew. Chem.* **1977**, *89*, 295–304.

[20] W. P. Jencks, *Adv. Enzymol. Relat. Areas Mol. Biol.* **1975**, *43*, 219–410.

[21] L. J. Hsu, N. S. Hsu, Y. L. Wang, C. J. Wu, T. L. Li, *Protein Eng. Des. Sel.* **2016**, *29*, 513–521.

Manuscript received: July 8, 2018

Accepted manuscript online: August 28, 2018

Version of record online: October 18, 2018

